

# Amphotericin B induces interdigitation of apolipoprotein stabilized nanodisk bilayers

Thanh-Son Nguyen<sup>a</sup>, Paul M.M. Weers<sup>b</sup>, Vincent Raussens<sup>c</sup>, Zhen Wang<sup>d</sup>, Gang Ren<sup>d</sup>,  
Todd Sulchek<sup>e</sup>, Paul D. Hoepflich Jr.<sup>e</sup>, Robert O. Ryan<sup>a,\*</sup>

<sup>a</sup> Center for Prevention of Obesity, Diabetes and Cardiovascular Disease, Children's Hospital Oakland Research Institute,  
5700 Martin Luther King Jr. Way, Oakland, CA 94609, USA

<sup>b</sup> Department of Chemistry and Biochemistry, California State University Long Beach, 1250 Bellflower Blvd, Long Beach, CA 90840, USA

<sup>c</sup> Center for Structural Biology and Bioinformatics, Laboratory for the Structure and Function of Biological Membranes,  
Université Libre de Bruxelles, Brussels, Belgium

<sup>d</sup> Department of Biochemistry & Biophysics, University of California, San Francisco,  
1700 4th Street, MC 2532, Byers Hall, Rm 301C, San Francisco, CA 94158, USA

<sup>e</sup> Chemistry, Materials & Lifesciences, Lawrence Livermore National Laboratory, 7000 East Avenue, P.O. Box 808, Livermore CA 94551, USA

Received 2 August 2007; received in revised form 19 September 2007; accepted 3 October 2007

Available online 16 October 2007

## Abstract

Amphotericin B nanodisks (AMB-ND) are ternary complexes of AMB, phospholipid and apolipoprotein organized as discrete nanometer scale disk-shaped bilayers. In gel filtration chromatography experiments, empty ND lacking AMB elute as a single population of particles with a molecular weight in the range of 200 kDa. AMB-ND formulated at a 4:1 phospholipid:AMB weight ratio separated into two peaks. One peak eluted at the position of control ND lacking AMB while the second peak, containing all of the AMB present in the original sample, eluted in the void volume. When ND prepared with increased AMB were subjected to gel filtration chromatography an increased proportion of phospholipid and apolipoprotein was recovered in the void volume with AMB. Native gradient gel electrophoresis corroborated the gel filtration chromatography data and electron microscopy studies revealed an AMB concentration-dependent heterogeneity in ND particle size. Stability studies revealed that introduction of AMB into ND decreases the ability of apoA-I to resist denaturation. Atomic force microscopy experiments showed that AMB induces compression of ND bilayer thickness while infrared spectroscopy analysis revealed that the presence of AMB does not induce extreme lipid disorder or alter the mean angle of the molecular axis along fatty acyl chains of ND phospholipids. Taken together the results are consistent with AMB-induced bilayer interdigitation, a phenomenon that likely contributes to AMB-dependent pore formation in susceptible membranes.

© 2007 Elsevier B.V. All rights reserved.

**Keywords:** Amphotericin B; Membrane; Nanodisk; Interdigitation; Atomic force microscopy; Infrared spectroscopy

## 1. Introduction

Amphotericin B (AMB) is a water insoluble macrolide polyene antibiotic that is widely used in the treatment of systemic fungal infections [1]. Recently, we reported a novel lipid formulation of AMB wherein the antibiotic integrates into

soluble nanometer scale, disk-shaped, apolipoprotein stabilized particles [2,3] referred to as nanodisks (ND). *In vitro* studies of AMB-ND revealed potent antifungal activity together with decreased toxicity toward erythrocytes and cultured hepatoma cells compared to AMB deoxycholate micelles [2]. Furthermore, *in vivo* efficacy studies in mice infected with either *Candida albicans* [2] or the protozoal parasite, *Leishmania major* [4] revealed that AMB-ND elicits strong antibiotic effects. Studies investigating the spectroscopic properties of AMB in ND revealed concentration and temperature dependent changes in spectral properties consistent with AMB self-association in the ND lipid milieu [3].

\* Corresponding author. Children's Hospital Oakland Research Institute, 5700 Martin Luther King Jr. Way, Oakland, CA 94609, USA. Tel.: +1 510 450 7645; fax: +1 510 450 7910.

E-mail address: [rryan@chori.org](mailto:rryan@chori.org) (R.O. Ryan).

A question that arises relates to whether AMB distributes among ND particles in a uniform manner or selectively partitions to create a population of AMB rich particles that co-exist with particles that lack AMB. At ratios of phospholipid:AMB used in the study by Hargreaves et al. [3] (4:1, 40:1 or 400:1 w/w), a uniform distribution model would require that AMB molecules be individually surrounded by phospholipid. Given the amphoteric nature of AMB and its propensity to self-associate [5], such a model seems unlikely.

In an effort to better define the molecular organization of AMB, phospholipid and apolipoprotein in AMB-ND, gel filtration chromatography, electrophoresis and electron/atomic force microscopy studies have been conducted. The data obtained indicate that, at high phospholipid:AMB weight ratios, AMB does not partition uniformly among ND particles but rather, combines with phospholipid at an optimal ratio to create a subpopulation of apolipoprotein stabilized particles that possess a ~1:1 phospholipid:AMB molar ratio. Increasing the starting AMB content to achieve a 1:1 phospholipid:AMB molar ratio results in generation of a population of larger diameter ND in which the bilayer is interdigitated.

## 2. Materials and methods

### 2.1. Materials

AMB (USP grade) was obtained from Research Organics Inc. Dimyristoyl-phosphatidylcholine (DMPC) was from Avanti Polar Lipids Inc. Recombinant apolipoprotein A-I (apoA-I) was produced as previously described [6].

### 2.2. AMB-ND preparation

Phospholipid vesicle dispersions were prepared as described earlier [2]. To the dispersed lipid a given amount of AMB from a stock solution (30 mg/ml in dimethylsulfoxide; DMSO) was added in a subdued light environment. Subsequent addition of apoA-I in buffer leads to a time-dependent decrease in sample turbidity with full sample clarity achieved by bath sonication with the sample temperature maintained at or below 25 °C. AMB-ND preparations contained 0, 2.5 or 12 mg AMB per 10 mg DMPC and 4 mg apolipoprotein. In the latter case, this corresponds to slightly higher than a 1:1 phospholipid:AMB molar ratio. When higher amounts of AMB were introduced to the reaction mix, precipitation occurred with loss of AMB. All preparations were dialyzed overnight at 4 °C and filter sterilized (0.22 μm) before use.

### 2.3. Gel filtration chromatography

Samples were applied to a 2.5 × 40 cm column of Sepharose 6B equilibrated in 0.1 M HEPES, pH 7.0, 150 mM NaCl and eluted in 2 ml fractions.

### 2.4. Circular dichroism spectroscopy

Far UV circular dichroism (CD) measurements were performed on a Jasco 810 spectropolarimeter to confirm the presence of α-helical structure in the various AMB-containing protein samples. For guanidine HCl denaturation experiments, samples (0.2 mg protein/ml) were incubated overnight in phosphate buffered saline at a given denaturant concentration in order to attain equilibrium, and ellipticity was measured at 222 nm (0.1 cm path length).

### 2.5. Analytical procedures

Protein concentrations were determined by the Bradford assay [7] with bovine serum albumin as standard. Native gradient PAGE was performed on 4–20% acrylamide slab gels and stained with Gel Code Blue (Pierce Chemical Co.). The

AMB content of samples was determined by transferring an aliquot to a solution of DMSO and measuring absorbance at 416 nm using an extinction coefficient =  $1.214 \times 10^5 \text{ M}^{-1} \text{ cm}^{-1}$  [2]. Choline containing phospholipids was quantified by enzyme based colorimetric assay (Wako) and phospholipid phosphorus content was quantitated as described by Bartlett [8].

### 2.6. Negative stain electron microscopy

Aliquots (2.5 μl) of ND samples were adhered to carbon-coated, 400 mesh copper grids previously rendered hydrophilic by glow discharge. The grids were washed for 1 min with three successive drops of deionized water and then exposed to three successive drops of 2% (w/v) uranyl nitrate for 1 min (Ted Pella, Tustin, CA). Images at 50,000× magnification were recorded on 4 K × 4 K Gatan UltraScan CCD under low electron dose conditions using a Tacnai 20 electron microscope (Philips Electron Optics/FEI, Eindhoven, The Netherlands) operating at 200 kV. Each pixel of the micrographs corresponds to 2.25 Å at the level of the specimen. Particles in micrographs were semi-automatically selected and boxed using EMAN software [9]. Each box size is 133 pixels, corresponding to 300 Å in specimen. In total, more than about 600 particles were selected and boxed from micrographs at each condition.

### 2.7. Atomic force microscopy

Atomic force microscopy (AFM) images were obtained with an Asylum Research MFP instrument. All images were acquired in aqueous tapping mode using silicon nitride cantilevers (0.1 N/m). Levers with blunt tips were discarded. All images were obtained in room temperature (~21 °C) aqueous solution. Samples were prepared by immobilizing ~2 μL solution of ND particles in imaging buffer (10 mM Tris-HCl (pH 8.0), 150 mM NaCl, and 10 mM MgCl<sub>2</sub>) onto a freshly cleaved mica surface and allowed to incubate for several minutes. Several rinse steps with imaging buffer followed. The topographies were post-processed with IgorPro software (WaveMetrics, Oregon) to remove first order slope in the line scans. Height and area histograms were calculated with custom software analysis and the data are given as mean ± SD. Images were false colored and sectioned to illustrate ND size.

### 2.8. Attenuated total reflectance Fourier transformed infrared spectroscopy (ATR-FTIR)

Spectra were recorded on a Bruker IFS 55 infrared spectrophotometer equipped with a reflectance accessory. The internal reflection element was a germanium crystal (50 × 20 × 2 mm) with an aperture angle of 45° yielding 25 internal reflections. 256 accumulations were performed to improve the signal/noise ratio. The spectrophotometer was continuously purged with dried air. Spectra were recorded at a nominal resolution of 2 cm<sup>-1</sup>. All measurements were made at room temperature. Oriented multilayers were formed by slow evaporation of ~15 μl of the different samples on one side of the ATR plate under a gentle stream of nitrogen, yielding a semi-dry film. For the determination of molecular orientations, spectra of lipids and/or ND complexes were recorded with parallel and perpendicular polarized incident light with respect to a normal to the ATR plate. Polarization was expressed as the dichroic ratio. The calculated dichroic ratio *R* is defined as the ratio of the band area recorded for the parallel polarization and perpendicular polarization. The ν<sub>as</sub>(CH<sub>2</sub>) and ν<sub>s</sub>(CH<sub>2</sub>) bands respectively at ~2919 and 2850 cm<sup>-1</sup>, whose dipole lies perpendicular to the hydrocarbon chains, was used to characterize lipid acyl chain orientation [10]. An estimation of the sample film thickness was obtained using the isotropic dichroic ratio, based on which the Order parameter (*S*) and angle for lipids with respect to a normal to the internal reflection element was estimated, taking into account the difference in the relative power of the evanescent field as described in [11]. The lipid ν(C=O) band around 1740 cm<sup>-1</sup> provides a good estimate for the isotropic dichroic ratio [12].

## 3. Results

### 3.1. Gel filtration chromatography studies

ND provide a lipid milieu capable of incorporating significant quantities of the water insoluble polyene antibiotic,

AMB [2,3]. The product particles are disk-shaped phospholipid–apolipoprotein complexes. The AMB component has been proposed to intercalate between phospholipid molecules in the disk bilayer. To gain insight into the structural organization of AMB, phospholipid and apolipoprotein in ND particles, gel filtration chromatography experiments were performed. ND lacking AMB eluted from a Sepharose 6B column as a single symmetrical peak of phospholipid and protein (data not shown). When ND formulated with 2.5 mg AMB or 12 mg AMB/10 mg DMPC and 4 mg apoA-I were applied to the column, 97% of the AMB eluted in the void volume (Fig. 1 upper panel). When the phospholipid content of the fractions was examined, in the case of ND generated with a 4:1 (w/w) DMPC:AMB ratio, 26% of the phospholipid mass

eluted in the void volume, with 74% recovered in fractions corresponding to empty ND (fractions 15–25). When the weight ratio of DMPC:AMB was changed to 10:12 (1:1 molar ratio), fully 90% the phospholipid eluted in the void volume (Fig. 1, middle panel). When the distribution of apoA-I was examined as a function of ND particle AMB content, 8% of apoA-I eluted in the void volume when ND were prepared at a 4:1 DMPC:AMB weight ratio, with the bulk of the protein (92%) eluting in a peak centered around fraction 20. On the other hand, in the case of ND formulated with 12 mg AMB per 10 mg DMPC, a larger proportion of the apoA-I eluted in the void volume (59%) with a substantial amount (41%) also eluting in a region of the profile corresponding to lipid-poor apoA-I (Fig. 1, lower panel).

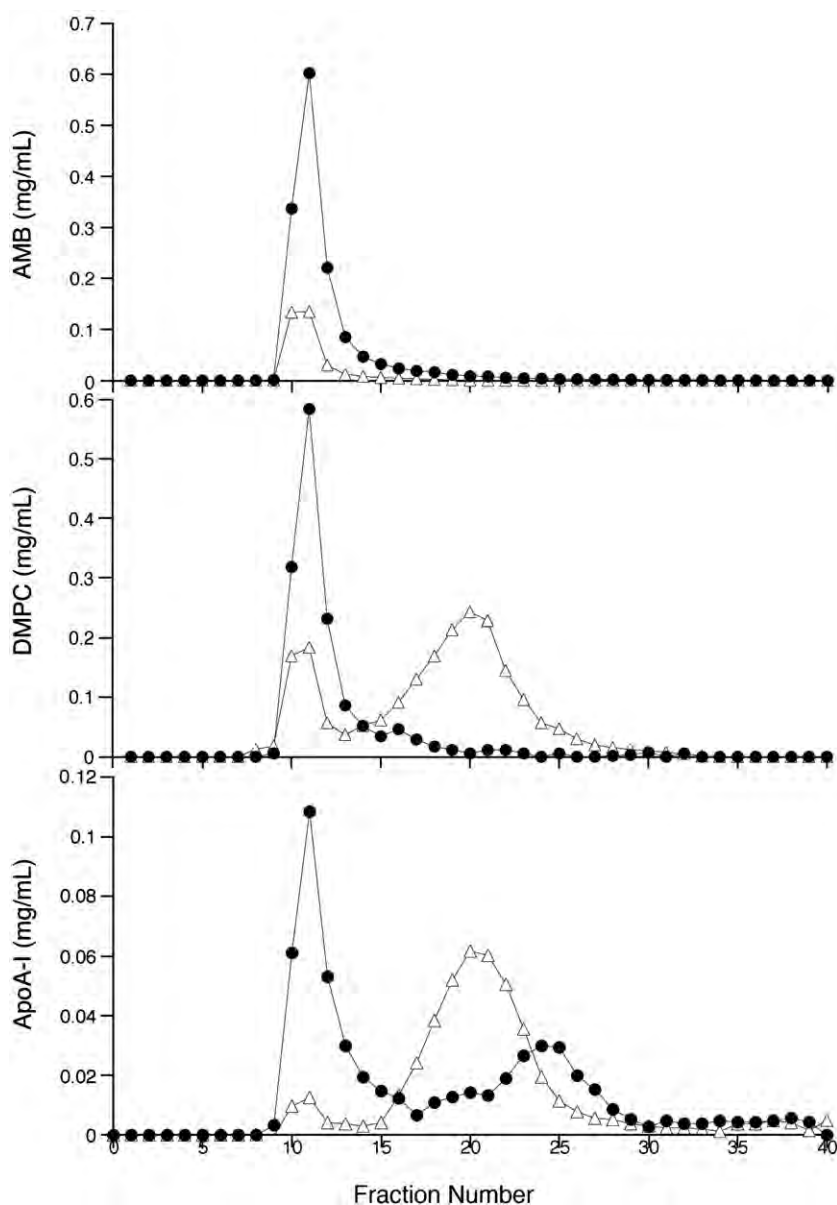


Fig. 1. Gel filtration chromatography of ND particles. AMB-ND prepared at AMB:DMPC:apoA-I weight ratios of 2.5:10:4 (open triangles) and 12:10:4 (filled circles) were applied to a Sepharose 6B gel filtration column and eluted in 2 ml fractions. The AMB content (upper panel), DMPC content (middle panel) and apolipoprotein content (lower panel) of each fraction was determined.

Based on these data we hypothesized that, during formation of ND, AMB does not distribute uniformly among the bulk phospholipid present, but rather, it selectively associates with ND phospholipid in a fixed stoichiometry such that AMB molecules interact both with other AMB and DMPC to achieve a preferred organizational state. At 2.5 mg AMB/10 mg DMPC the system contains phospholipid mass in excess of that required to achieve the preferred AMB–DMPC molecular organization. In this case excess DMPC exists in complexes with apoA-I as empty ND. An apparent intrinsic difference in behavior of these co-existing populations of particles is revealed by gel permeation chromatography of the sample. A further observation is that, prior to gel permeation chromatography, AMB-ND preparations could be filtered through a 0.22  $\mu\text{m}$  membrane without loss of AMB. By contrast, after gel permeation chromatography the voided material, which contains all of the AMB present in the original sample, could not be filtered through a 0.22  $\mu\text{m}$  membrane. Taken together, these data suggest that AMB solubilized in ND aggregates upon gel permeation chromatography resulting in its separation from the bulk of the lipid and apolipoprotein, which remain as discrete ND particles. From the composition of the voided material, it appears that AMB selectively associates with itself in a preferred ratio with phospholipid and small amounts of apoA-I to generate large AMB–DMPC aggregates.

If AMB selectively interacts with a fixed amount of DMPC (generating particles with an approximate 1:1 DMPC:AMB molar ratio), then the maximum amount of AMB that can be solubilized by incorporation into ND should correspond to a 1:1 molar ratio of these components (AMB molecular weight=924 g/mol; DMPC molecular weight=678 g/mol). Consistent with this we found that approximately 12 mg AMB can be solubilized by 10 mg DMPC and 4 mg apoA-I, an amount far greater than the 2.5 mg AMB per 10 mg DMPC mass reported earlier [2]. In the case of ND prepared with 12 mg AMB per 10 mg DMPC, gel filtration results in elution of all of the AMB and phospholipid present in the sample in the void volume with apoA-I distributed between the voided fraction and a later eluting fraction that corresponds to free apoA-I. Again, although AMB recovered from the gel filtration column following chromatography of these ND was soluble in buffer, it could not be filtered through a 0.22  $\mu\text{m}$  filter. These data support the concept that AMB interacts with phospholipid in an optimal ratio to generate a population of ND particles that are enriched in AMB and are protected from aggregation by apoA-I. The reason why AMB–DMPC–apoA-I complexes, but not DMPC–apoA-I complexes (empty ND) are susceptible to fusion/aggregation upon gel filtration chromatography is unclear but appears to involve apoA-I dissociation from the ND surface.

A trivial explanation for the observed results is that AMB-ND are intrinsically unstable and apparent aggregation of this sample is not dependent upon gel filtration or other perturbation of the system. To test this particle integrity and AMB solubility was examined as a function of time. At time 0 a 0.5 ml aliquot of AMB-ND (4:1 weight ratio of DMPC:AMB) was passed through a 0.22  $\mu\text{m}$  membrane filter with recovery of 84% of the

original AMB. Following 5 days storage at 4 °C in buffer a separate 0.5 ml aliquot was passed through a 0.22  $\mu\text{m}$  membrane filter. In this case the recovery of AMB was 82%. Furthermore, no precipitate formed in the sample.

### 3.2. Native PAGE studies

Native gradient PAGE of AMB-ND prepared at a 4:1 weight ratio of DMPC:AMB revealed a discrete population of particles with a diameter in the range of 8.5 nm [2]. On the basis of the gel filtration results described above, however, it is conceivable that electrophoretic separation may induce a similar alteration in AMB-containing particles. Native PAGE analysis of ND prepared with increasing amounts of AMB revealed an AMB concentration-dependent decrease in the intensity of the ND band migrating at 8.5 nm (Fig. 2). Accompanying this was a corresponding increase in the amount of apparently aggregated material that did not enter the gel. Furthermore, the AMB concentration-dependent decline in the 8.5 nm particle band was accompanied by the appearance of a band corresponding to lipid-poor apoA-I. To determine if the aggregated material recovered at the top of the gel contains AMB, the gel was directly visualized without staining (Fig. 2, panel B). This region, and only this region, of the unstained gel showed a distinct yellow hue, consistent with the color of AMB. Thus, we conclude that AMB-containing ND particles coalesce during native gel electrophoresis in a manner similar to that observed during gel filtration chromatography.

### 3.3. Negative stain electron microscopy of ND samples

Consistent with observations described above, electron microscopy of the material eluting in the void volume following gel filtration chromatography of AMB-ND revealed a population

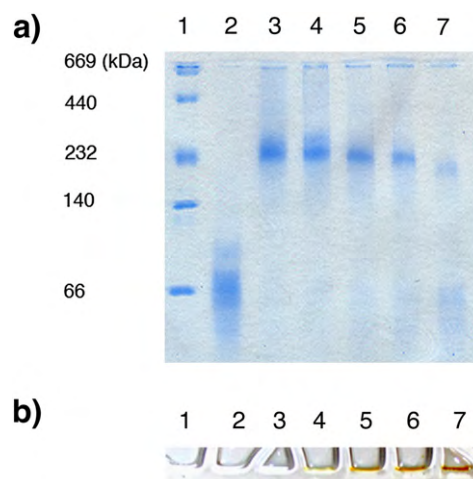


Fig. 2. Native gradient PAGE of ND. Samples were applied to a 4–20% acrylamide, Tris–glycine slab gel and electrophoresed for 24 h at 150 mV. Lane 1) Molecular weight standards; lane 2) lipid free A-I; lane 3) empty ND lane 4) AMB-ND (2.5 mg AMB/10 mg DMPC); lane 5) AMB-ND (6 mg AMB per 10 mg DMPC); lane 6) AMB-ND (9 mg AMB per 10 mg DMPC) and lane 7) AMB-ND (12 mg AMB per 10 mg DMPC). Lower panel; same gel as above but not stained for protein.

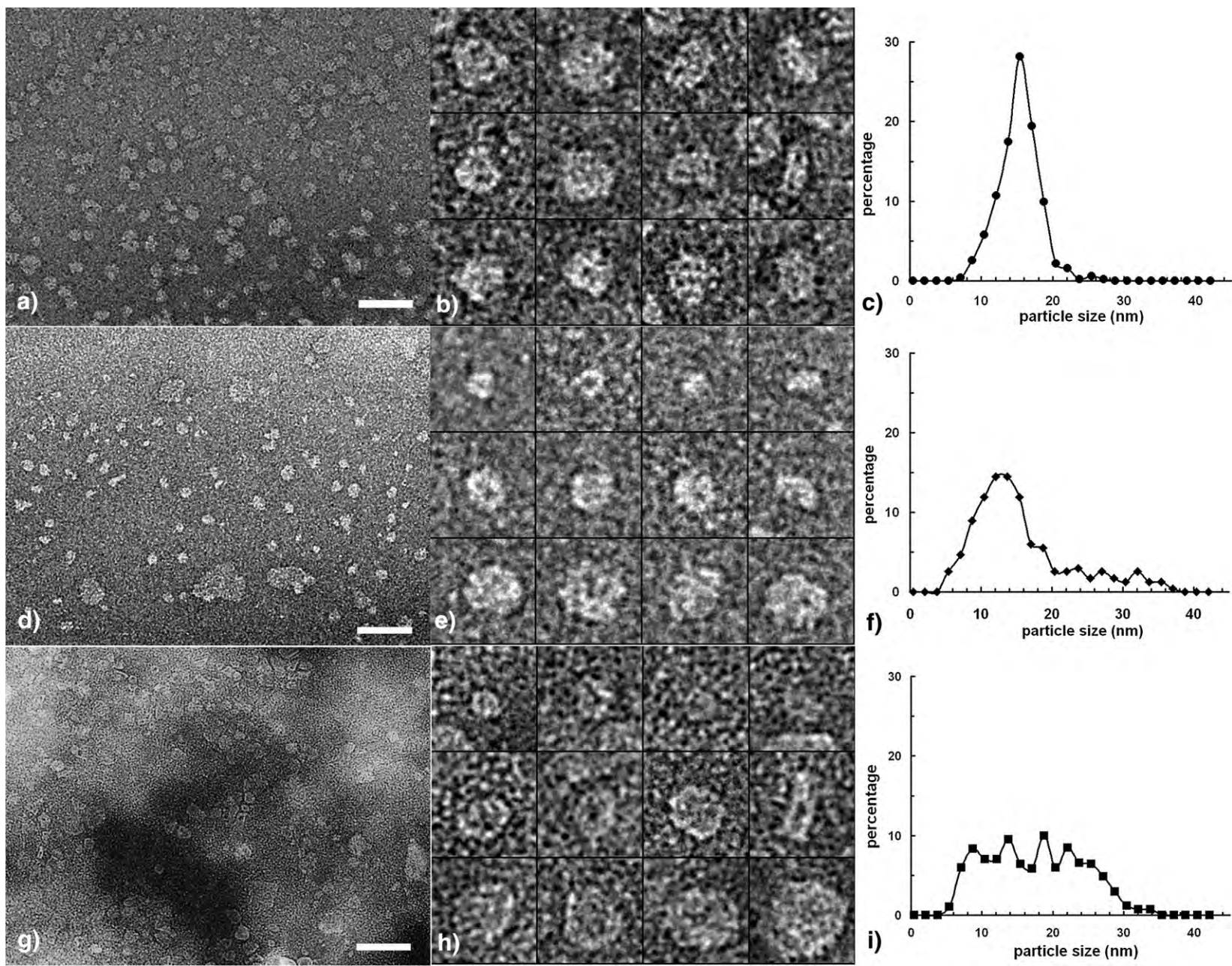


Fig. 3. Negative stain electron microscopy of ND. Wide field micrographs of empty ND (panel a), AMB-ND prepared at 5 mg AMB/10 mg DMPC (w/w) (panel d) and AMB-ND prepared at 12 mg AMB/10 mg DMPC (w/w) (panel g). In each case the bar corresponds to 60 nm. Individual particle size and morphology were examined in panels b, e and h (each box corresponds to 30 nm). Panels c, f and i are plots of particle diameter versus particle number for empty ND (panel c), AMB-ND prepared at 5 mg AMB/10 mg DMPC (w/w) (panel f) and AMB-ND prepared at 12 mg AMB/10 mg DMPC (w/w) (panel i). Each plot is based on a minimum 600 individual particle size measurements.

of aggregated particles with diameters of  $\sim 0.5 \mu\text{m}$  (data not shown). To investigate the effect of AMB on ND size and morphology prior to any modifications induced by gel filtration or electrophoresis, negative stain electron microscopy (EM) was performed on freshly prepared ND samples. As expected, empty ND showed a uniform particle size distribution (Fig. 3) with 70% of ND particle diameters in the range of 14–17 nm. By contrast, ND prepared with 5 mg AMB per 10 mg DMPC displayed particle size heterogeneity. This sample was comprised of a spectrum of particles that were both larger and smaller than the average empty ND (Fig. 3, panels d, e, f). When an even higher amount of AMB was present (12.5 mg per 10 mg DMPC), greater particle size heterogeneity was observed (Fig. 3, panels g, h, i), ranging from small ( $<10 \text{ nm}$ ) to large ( $>25 \text{ nm}$ ). The number of particles with a diameter in the range of 14–17 nm decreased from 70% in empty ND to 30% and 22% in ND prepared with 5 mg AMB and 12.5 mg AMB, respectively. At the same time introduction of AMB increased the number of larger diameter particles (size range 20–25 nm) from 3% of the population to 12% and 25%, respectively. Likewise, the number of smaller diameter particles, perhaps corresponding to lipid-poor apoA-I (8–11 nm), increased from 9% to 25%. These data strongly suggest that AMB induces structural changes in ND particles that are manifested by greater particle size heterogeneity as well as susceptibility to aggregation upon gel filtration or native gel electrophoresis.

### 3.4. Circular dichroism spectroscopy studies

To evaluate whether AMB-ND are intrinsically less stable than control ND lacking AMB, denaturation experiments were conducted. The effect of guanidine HCl on the secondary structure of the apoA-I component of ND was evaluated by CD spectroscopy as a function of AMB content (Fig. 4). Consistent with previous studies, association of apoA-I with DMPC to create ND confers considerable stability to this protein [13]. Whereas lipid free apoA-I gave rise to a denaturation transition midpoint of 1 M guanidine HCl, the corresponding value for

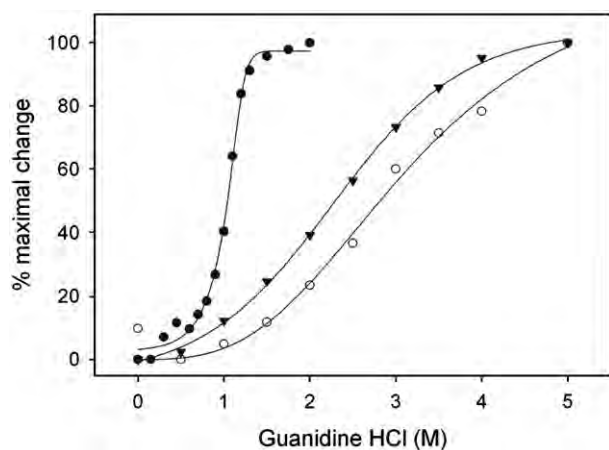


Fig. 4. Effect of guanidine HCl on apoA-I stability. The secondary structure content of apoA-I in buffer (solid circles), in empty ND (e.g. DMPC only; open circles) and in AMB-ND (2.5 mg AMB per 10 mg DMPC; closed inverted triangles) was measured by far UV CD spectroscopy. Sample ellipticity at 222 nm was determined at the indicated denaturant concentrations.

apoA-I associated with empty ND was  $\sim 3 \text{ M}$ . Incorporation of small amounts of AMB (0.25 mg AMB per 10 mg DMPC) had no discernable effect on apoA-I stability while increasing the AMB content to 20% of the lipid mass (2.5 mg AMB per 10 mg DMPC) induced a shift in apoA-I denaturation profile, yielding a transition midpoint of 2.3 M guanidine HCl. Attempts to measure ND with increased AMB contents failed due to interference by AMB with the spectroscopic analysis. These data show that inclusion of AMB in ND affects the ability of apoA-I to resist denaturation, a result that correlates with the apparent dissociation of apoA-I during gel filtration or electrophoresis.

### 3.5. Atomic force microscopy of ND

To further examine the effects of AMB on ND structure, AFM experiments were conducted. AFM images like scanning electron microscopy except that it scans a tip over the surface and monitors surface topography in a physiological environment (Fig. 5, panel a). Images of empty ND at high concentration revealed close packing of the disks that gave rise to a measured diameter of  $11.1 \pm 2.1 \text{ nm}$  (Fig. 5, panels a, b), in good agreement with values obtained by negative stain EM and non-denaturing gradient gel electrophoresis. At lower ND concentrations, individual particles were visualized (Fig. 5, panel c). The height of the disks was observed to be  $5.2 \pm 0.4 \text{ nm}$  (Fig. 5, panel f), consistent with the thickness of a DMPC bilayer [14]. Introduction of a high concentration of AMB (12 mg AMB per 10 mg DMPC) had two major effects on this system (Fig. 5, panels d, g). The diameter of most particles increased to  $\sim 35 \pm 15 \text{ nm}$  with a few particles observed with a diameter similar or less than that of empty ND. At the same time, the height of the disks was reduced. The largest reduction in height was observed in the center of the particles ( $2.5 \pm 0.4 \text{ nm}$ ) while the perimeter of the particles was  $\sim 3.4 \pm 0.6 \text{ nm}$  in height. Height values were force independent such that changing the force of imaging had little effect on the absolute particle height values. To further investigate the effect of AMB on ND particle size and structure, particles were prepared that contained an intermediate AMB content (2.5 mg AMB per 10 mg DMPC). Under this condition evidence for the co-existence of two particle populations was obtained (Fig. 5, panels e, h). One population displayed particle diameter and height characteristics similar to that of empty ND while the second population was similar in size and height to ND prepared with the maximal AMB content.

### 3.6. Infrared spectroscopy analysis

Previous work by others has shown that FTIR analysis is well suited to studies of AMB in a lipid environment [15]. In the present context, we evaluated the effect of AMB incorporation on the organizational state of the DMPC and apoA-I components of ND by ATR-FTIR (Table 1). Whereas DMPC alone gave rise to relatively high  $S$  values, the Order parameter for DMPC decreased when present in a ND membrane environment. Interestingly, upon addition of AMB, the Order parameter

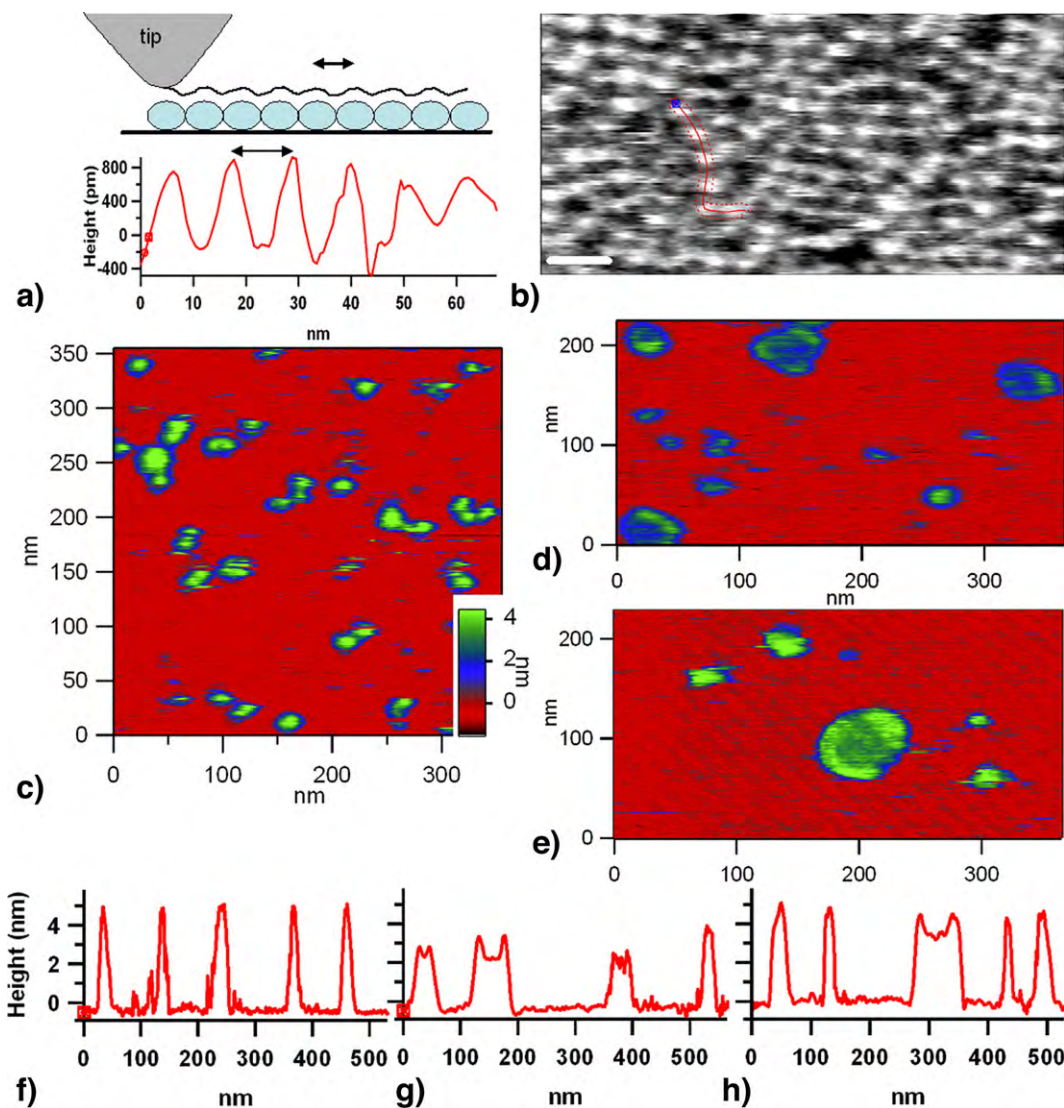


Fig. 5. Atomic force microscopy of ND. Panel a, upper portion) diagram of tip surface probe; lower portion) tip probe measurement of empty ND particle height. Panel b) image of empty ND at high concentration (white scale bar=25 nm); panels c–e) AFM images of ND at low concentration including empty ND (panel c); AMB-ND prepared at 12 mg AMB/10 mg DMPC (w/w) (panel d) and AMB-ND prepared at 2.5 mg AMB/10 mg DMPC (panel e). Panels f–h) tip probe measurements of ND imaged in panels c, d and e, respectively.

increased, suggesting the observed membrane thinning is not the result of AMB-induced lipid disorder. Likewise, only minor differences were observed in the width of lipid specific peaks and DMPC orientation angle as a function of incorporation into ND or upon inclusion of AMB. In analysis of dichroic spectra, it was observed that, in both empty ND and AMB-ND, the long axis of apoA-I  $\alpha$ -helices align perpendicular to the DMPC fatty acyl chains, as previously shown [16]. Furthermore, estimation of the secondary structure content of apoA-I in empty ND and AMB-ND revealed 60% and 59% alpha helix content, respectively. Thus, these data show that AMB incorporation does not alter the fundamental structural organization of the ND particle or its apolipoprotein scaffold.

#### 4. Discussion

We recently reported the generation of apolipoprotein stabilized, nanoscale sized bilayer disks that possess significant

quantities of the amphiphilic macrolide polyene antibiotic, AMB [2,3]. Interest in these particles has been generated by the observation that AMB-ND show efficacy in a mouse model of candidiasis with low toxicity toward red blood cells and cultured hepatoma cells. Recently, AMB-ND was shown to be highly effective in the treatment of cutaneous *Leishmania major* infection in BALB/c mice [4]. In considering the molecular basis for the apparent enhanced efficacy of AMB-ND, questions exist about the distribution of AMB among ND particles and the nature of the interaction of AMB with other ND particle components. Moreover, the mechanism of action of this antifungal agent remains uncertain. How this 924 Da amphoteric molecule forms a bilayer spanning pore has not been definitively determined. Knowledge of the effect of AMB on phospholipids will provide a valuable clue as to this action.

In the present study we took advantage of the phospholipid solubilization properties of recombinant human apoA-I to form discrete ternary complexes of AMB, phospholipid and

Table 1  
Mean orientation angles ( $\theta$ ) and spectral characteristics of CH<sub>2</sub> vibration along the acyl chains of lipids using linear dichroism experiments by ATR-FTIR

	Vibration	Band position (cm <sup>-1</sup> )	FWHH <sup>a</sup>	Dichroic ratio $R^b$	$S^c$	$\theta$ (°) <sup>d</sup>
DMPC	$\nu_s(\text{CH}_2)$	2915	17.4	1.10	0.82	29
	$\nu_{as}(\text{CH}_2)$	2848	9.1	1.10	0.80	30
ND	$\nu_s(\text{CH}_2)$	2919	20.4	1.47	0.44	34
	$\nu_{as}(\text{CH}_2)$	2848	10.4	1.46	0.44	34
AMB-ND <sup>e</sup>	$\nu_s(\text{CH}_2)$	2919	21.8	1.18	0.67	32
	$\nu_{as}(\text{CH}_2)$	2848	10.2	1.14	0.80	28

<sup>a</sup> Full width at half height.

<sup>b</sup> Measured dichroic ratios using linearly polarized IR light.

<sup>c</sup> Order parameters were obtained using the corresponding dichroic ratio and electric field amplitudes for intermediate film thickness as described [19]; the corresponding isodichroic ratios are respectively 1.29, 1.56, and 1.34 for DMPC, ND, and AMB-ND. The estimated error on this parameter is  $\sim 0.05$ .

<sup>d</sup> Mean angle of the molecular axis along the acyl chains with a normal to the internal reflection element. The error on the calculated angle is estimated to be  $< 5^\circ$ .

<sup>e</sup> Particles contained a 1:1 molar ratio of AMB:DMPC.

apolipoprotein. Given the high content of AMB that can be fully solubilized in these particles (up to a 1:1 molar ratio with DMPC), it is likely that a repeating AMB–DMPC structural organization exists. As with non-AMB-containing bilayer disks, it is envisioned that apoA-I molecules circumscribe the perimeter of the complexes in such a manner that the hydrophobic faces of their amphipathic  $\alpha$ -helices are in contact with phospholipid fatty acyl chains (or AMB molecules) at the disk edge. In the case of non-AMB-containing ND such a model is supported by a large body of evidence including infrared spectroscopy, fluorescence resonance energy transfer and electron paramagnetic resonance spectroscopy [16–18]. Such empty ND complexes are quite stable and can be sized by gel filtration chromatography, non-denaturing PAGE or EM. By contrast, introduction of AMB into ND particles has a major effect on the behavior of the particles, consistent with AMB-induced fusion of egg yolk PC liposomes observed by Gabrielska et al. [19]. Gel filtration chromatography studies reveal a propensity of AMB to self-associate/aggregate resulting in antibiotic elution in the column void volume along with a fixed amount of phospholipid and a lesser amount of protein. Two important conclusions can be drawn from these results. First, when prepared at a  $>1:1$  molar ratio of phospholipid:AMB, AMB does not partition equally into ND particles. Instead, AMB associates with DMPC to generate a repeating structural organization that possesses a 1:1 phospholipid:AMB molar ratio. This property was also observed by Janoff et al. [20], who reported that mixtures of AMB, DMPC and dimyristoylphosphatidylglycerol form extended ribbon-like structures that, upon sucrose density gradient centrifugation, results in freezing out of AMB from the bulk of the phospholipid. Second, apoA-I associated with ND particles that contain AMB and DMPC in this organizational state is less stably associated with the particle than apoA-I associated with ND that lack AMB. Based on this behavior, we suspected that, at a starting DMPC:AMB weight ratio of 4:1, two populations of ND are formed, those that contain AMB and DMPC in a 1:1

molar ratio and those that contain the remainder of the DMPC without AMB. While native gel electrophoresis experiments support this view, negative stain EM permitted direct visualization of the effect of AMB on ND particle size heterogeneity. Whereas studies reported earlier [2] suggested AMB-containing ND are similar to “empty” ND, it must be recognized that, given the present interpretation, the major component in the sample employed by Oda et al. [2] corresponds to empty ND, with at most 20% of the ND containing AMB. Indeed, on further analysis (Figs. 3, 5) direct evidence that AMB induces ND particle size heterogeneity has been obtained.

Focusing on the curious finding that, upon gel filtration chromatography of AMB-ND, apoA-I dissociates from the particle, we evaluated the stability of ND associated apoA-I. Guanidine HCl denaturation studies revealed that the presence of AMB in ND particles causes a decrease in apoA-I stability consistent with the hypothesis that apoA-I dissociates at lower guanidine HCl than when associated with empty ND. Subsequent atomic force microscopy experiments provided a plausible explanation for this result. Introduction of AMB at a  $\sim 1:1$  molar ratio with DMPC generated a population of ND particles that were of larger diameter and reduced height compared to control empty ND. The larger diameter of the AMB-containing ND confirmed data obtained by negative stain EM and suggests they contain more than the two apoA-I molecules normally associated with empty ND. Based on infrared spectroscopy analysis, this association likely involves an extended “belt” conformation for apoA-I, with its helical segments aligned perpendicular to the fatty acyl chains of DMPC [16,21]. AFM of ND yielded a bilayer thickness of about 5 nm, consistent with values reported by others [14]. By contrast, the height of larger diameter AMB-containing particles was 2.5 nm in the center and between 3.0 and 4.0 nm at the edge of the particle.

Given that the phospholipid component of empty ND is generally considered to exist as a bilayer, the present data could arise if AMB-induced extreme disorder that is manifest as membrane thinning. ATR-FTIR spectroscopy analysis, however, yielded tilt angle and Order parameter values for the DMPC component that are not consistent with membrane thinning due to disorder. Based on this data, we suggest AMB intercalation perturbs the bilayer so as to interdigitate the phospholipid fatty acyl chains. In an interdigitated bilayer the hydrocarbon chains of phospholipids in opposing leaflets interpenetrate [22]. In general, slippage of fatty acyl chains of a given phospholipid against corresponding phospholipid fatty acyl chains in the opposite leaflet of the bilayer can be induced by pressure or small amphiphilic molecules such as the short chain alcohols ethanol or benzyl alcohol [23]. In addition, amphiphilic agents such as atropine have been shown to induce bilayer interdigitation [24]. In the case of ND membranes, bilayer interdigitation would be expected to have an effect on the association of apolipoprotein around the perimeter of the disk. Compression of the bilayer thickness may hinder apolipoprotein interaction, resulting in greater likelihood of dissociation compared to ND of normal bilayer thickness (e.g. empty ND). The observation that the edge of AMB-containing disks are  $\sim 1$  nm thicker than

the central region of the disk may indicate that the perimeter of the disk is circumscribed by multiple apoA-I molecules that align in tandem. In this manner the edge of the disk would resist compression upon AMB-induced phospholipid interdigitation although the stability of apoA-I association with the particle may be decreased. Thus, AMB-dependent bilayer interdigitation can explain the loss of apoA-I from the ND particles upon gel filtration or electrophoresis and this occurrence would likely promote fusion of residual AMB–DMPC, creating the large aggregates that elute in the void volume following gel filtration chromatography.

The finding that AMB is capable of inducing ND bilayer interdigitation has important implications in terms of the mechanism of action of this potent antifungal agent. It is generally accepted that AMB interaction with itself and membrane sterols leads to pore formation that results in leakage of cell contents and cell death. The higher activity of AMB toward fungal cell membranes has been ascribed to a preferred interaction with ergosterol versus cholesterol present in mammalian cell membranes [1]. While the precise organization of AMB membrane pores is not known, two prevailing models exist. In one model AMB forms a “half-pore” in one leaflet of the bilayer, with a functional pore occurring when two half-pores, in opposite leaflets of the bilayer, join one another to make a double pore that spans the bilayer width. In a second model, suggested to exist in egg phosphatidylcholine bilayers, AMB forms a functional half-pore that results from a local compression of the bilayer width [25,26]. This latter model may be explained on the basis of AMB-induced membrane interdigitation. Interdigitation of a target membrane will decrease bilayer thickness such that a pore that is the length of an AMB molecule may span the membrane. Another key factor in the process of AMB-induced membrane pore formation is its propensity to self-associate. It is postulated that AMB pores are comprised of 8–12 AMB molecules complexed with an equivalent number of membrane sterols, presumably via their hydrophobic polyene face such that the interior diameter of the resulting hydrophilic pore would allow unrestricted ion movement. Thus, AMB self-association, interaction with sterols and ability to induce bilayer interdigitation appear to represent critical aspects of membrane pore formation that give rise to the biological activity of this, and most likely, other members of the large family of macrolide polyene antibiotics.

## Acknowledgments

This work was supported by grants from the National Institutes of Health (AI-162541 and AI-061354). G.R. was supported by funds from the W.M. Keck Advanced Microscopy Laboratory at UCSF. V.R. is a Research Associate at the National Fund for Scientific Research (Belgium). T.S. and P.D. H. acknowledge support from the Livermore Laboratory Science and Technology Office under 06-SI-003. This work was performed under the auspices of the United States Department of Energy by the University of California, Lawrence Livermore National Laboratory under contract number W-7405-ENG-48 (UCRL-JRNL-226688). P.M.M.W.

was supported by the National Institutes of Health Minority Biomedical Research Support Program Support of Continuous Research Excellence grant (GM-063119).

## References

- [1] S. Hartsel, J. Bolard, Amphotericin B: new life for an old drug, *Trends Pharmacol. Sci.* 17 (1996) 445–449.
- [2] M.N. Oda, P.L. Hargreaves, J.A. Beckstead, K.A. Redmond, R. van Antwerpen, R.O. Ryan, Reconstituted high-density lipoprotein enriched with the polyene antibiotic, amphotericin B, *J. Lipid Res.* 47 (2006) 260–267.
- [3] P.L. Hargreaves, T.-S. Nguyen, R.O. Ryan, Spectroscopic studies of amphotericin B solubilized in nanoscale bilayer membranes, *Biochim. Biophys. Acta* 1758 (2006) 38–44.
- [4] K.G. Nelson, J. Bishop, R.O. Ryan, R. Titus, Nanodisk-associated amphotericin B clears *Leishmania major* cutaneous infection in susceptible BALB/c mice, *Antimicrob. Agents Chemother.* 50 (2006) 1238–1244.
- [5] J. Barwicz, P. Tancrede, The effect of aggregation state of amphotericin-B on its interactions with cholesterol- or ergosterol-containing phosphatidylcholine monolayers, *Chem. Phys. Lipids* 85 (1997) 145–155.
- [6] R.O. Ryan, T.M. Forte, M.N. Oda, Optimized bacterial expression of human apolipoprotein A-I, *Protein Expr. Purif.* 27 (2003) 98–103.
- [7] M.M. Bradford, A rapid and sensitive method for the quantitation of microgram quantities of protein utilizing the principle of protein-dye binding, *Anal. Biochem.* 72 (1976) 248–254.
- [8] G.R. Bartlett, Colorimetric assay methods for free and phosphorylated glyceric acids, *J. Biol. Chem.* 234 (1959) 469–471.
- [9] J. Ludtke, P.R. Baldwin, W. Chiu, EMAN: semiautomated software for high-resolution single-particle reconstructions, *J. Struct. Biol.* 128 (1999) 82–97.
- [10] U.P. Fringeli, H.H. Gunthard, Infrared membrane spectroscopy, *Mol. Biol. Biochem. Biophys.* 31 (1981) 270–332.
- [11] E. Goormaghtigh, V. Raussens, J.M. Ruyschaert, Attenuated total reflection infrared spectroscopy of proteins and lipids in biological membranes, *Biochim. Biophys. Acta* 1422 (1999) 105–185.
- [12] B. Bechinger, J.-M. Ruyschaert, E. Goormaghtigh, Membrane helix orientation from linear dichroism of infrared attenuated total reflection spectra, *Biophys. J.* 76 (1999) 552–563.
- [13] D.J. Reijngoud, M.C. Phillips, Mechanism of dissociation of human apolipoprotein A-I from complexes with dimyristoylphosphatidylcholine as studied by guanidine hydrochloride denaturation, *Biochemistry* 21 (1982) 2969–2976.
- [14] O. Enders, A. Ngezahayo, M. Wiechmann, F. Leisten, H.A. Kolb, Structural calorimetry of main transition of supported DMPC bilayers by temperature-controlled AFM, *Biophys. J.* 87 (2004) 2522–2531.
- [15] M. Gagos, J. Gabrielska, M. Dalla Serra, W.I. Gruszecki, Binding of antibiotic amphotericin B to lipid membranes: monomolecular layer technique and linear dichroism-FTIR studies, *Molec. Memb. Biol.* 22 (2005) 433–442.
- [16] V. Koppaka, L. Silvestro, J.A. Engler, C.G. Brouillette, P.H. Axelsen, The structure of human lipoprotein A-I. Evidence for the “belt” model, *J. Biol. Chem.* 274 (1999) 14541–14544.
- [17] M.N. Oda, T.M. Forte, R.O. Ryan, J.C. Voss, The C-terminal domain of apolipoprotein A-I contains a lipid sensitive conformational trigger, *Nature Struct. Biol.* 10 (2003) 455–460.
- [18] D.D.O. Martin, M.S. Budamagunta, R.O. Ryan, J.C. Voss, M.N. Oda, Apolipoprotein A-I assumes a “looped belt” conformation on reconstituted high density lipoprotein, *J. Biol. Chem.* 281 (2006) 20418–20426.
- [19] J. Gabrielska, M. Gagos, J. Gubernator, W.I. Gruszecki, Binding of antibiotic amphotericin B to lipid membranes: a 1H NMR study, *FEBS Lett.* 580 (2006) 2677–2685.
- [20] A.S. Janoff, L.T. Boni, M.C. Popescu, S.R. Minchey, P.R. Cullis, T.D. Madden, T. Taraschi, S.M. Gruner, E. Shyamsunder, M.W. Tate, R. Mendelsohn, D. Bonner, Unusual lipid structures selectively reduce the toxicity of amphotericin B, *Proc. Natl. Acad. Sci. U. S. A.* 85 (1988) 6122–6126.
- [21] W.S. Davidson, R.A. Silva, Apolipoprotein structural organization in high density lipoproteins: belts, bundles, hinges and hairpins, *Curr. Opin. Lipidol.* 16 (2005) 295–300.

- [22] J.L. Slater, C-H. Huang, Interdigitated bilayer membranes, *Prog. Lipid Res.* 27 (1988) 325–359.
- [23] M. Kranenburg, M. Vlaar, B. Smit, Simulating induced interdigitation in membranes, *Biophys. J.* 87 (2004) 1596–1605.
- [24] Y.H. Hao, Y.M. Xu, Chen, F. Huang, A drug–lipid interaction model: atropine induces interdigitated bilayer structure, *Biochem. Biophys. Res. Commun.* 245 (1998) 439–442.
- [25] B. De Kruijff, R.A. Demel, Polyene antibiotic–sterol interactions in membranes of *acholeplasma laidlawii* cells and lecithin liposomes. 3. Molecular structure of the polyene antibiotic–cholesterol complexes, *Biochem. Biophys. Acta* 339 (1974) 57–70.
- [26] A. Marty, A. Finkelstein, Pores formed in lipid bilayer membranes by nystatin, differences in its one-sided and two-sided action, *J. Gen. Physiol.* 65 (1975) 515–526.